ELSEVIER

Physica B 307 (2001) 125–137

PHYSICA B

www.elsevier.com/locate/physb

Doping dependence of the barrier height and ideality factor of Au/n-GaAs Schottky diodes at low temperatures

M.K. Hudait[a,b,*], S.B. Krupanidhi[a]

[a] *Materials Research Centre, Indian Institute of Science, Bangalore-560 012, India*
[b] *Central Research Laboratory, Bharat Electronics, Bangalore-560 013, India*

Received 18 October 1999; received in revised form 28 February 2001; accepted 26 June 2001

Abstract

The barrier height and ideality factor of Au/n-GaAs Schottky diodes grown by metal-organic vapor-phase epitaxy (MOVPE) on undoped and Si-doped n-GaAs substrates were determined in the doping range of 2.5×10^{15}–$1\times10^{18}\,cm^{-3}$ at low temperatures. The thermionic-emission zero-bias barrier height for current transport decreases rapidly at concentrations greater than $1\times10^{18}\,cm^{-3}$. The ideality factor also increases very rapidly at higher concentration and at lower temperature. The results agree quite well with thermionic field emission (TFE) theory. The doping dependence of the barrier height and the ideality factor were obtained in the concentration range of 2.5×10^{15}–$1.0\times10^{18}\,cm^{-3}$ and the results are well described using TFE theory. An excellent match between the homogeneous barrier height and the effective barrier height was observed which supports the good quality of the GaAs film. The observed variation in the zero-bias barrier height and the ideality factor can also be explained in terms of barrier height inhomogeneities in the Schottky diode.

Keywords: Schottky barrier; Gallium arsenide; Metal-organic vapor-phase epitaxy; Electrical measurements

1. Introduction

Electrical transport in Schottky diodes on epi-GaAs grown on n-GaAs substrates has been of considerable interest for the past several years. For electronic and optoelectronic devices made by compound semiconductors, the Schottky contact plays an important role in the performance of its associated devices. The performance and reliability of a Schottky diode is drastically influenced by the interface quality between the deposited metal and the semiconductor surface. Schottky barrier diodes (SBDs) have been widely studied and many attempts have been made to understand the conduction mechanism across such Schottky diodes. The knowledge of the conduction mechanism across a Schottky barrier is essential in order to calculate the Schottky barrier parameters and explain the observed effects. Generally, the SBD parameters are determined over a wide range of temperatures and doping concentrations in order to understand the nature of the barrier and the conduction mechanism. Thermionic emission (TE) theory is normally used to extract the SBD

*Corresponding author. Present address: Department of Electrical Engineering, The Ohio State University, Columbus, OH 43210, USA. Tel.: +1-614-292-1721; fax: +1-614-292-7596.

E-mail address: hudaitm@ee.eng.ohio-state.edu (M.K. Hudait).

0921-4526/01/$ -see front matter
PII: S0921-4526(01)00631-7

parameters [1–7], however, there have been several reports of certain anomalies [4,7–9] at low temperatures. The ideality factor and barrier height determined from the forward bias current–voltage ($I-V$) characteristics on the basis of the TE mechanism were found to be a strong function of temperature and doping concentration [5,9–20].

The ideality factor was found to increase with decreasing temperature and increasing carrier concentration. The increase in ideality factor with decreasing temperature is known as the T_0 effect and was first reported by Padovani and Sumner [2]. The Schottky barrier height (SBH), Φ_{I-V} measured by the $I-V$ technique for TE decreases with decreasing temperature and increasing doping level, while the SBH Φ_{C-V} measured by the capacitance–voltage ($C-V$) method remains constant. The SBH determined depends on the technique of measurement; typically, Φ_{C-V} significantly exceeds Φ_{I-V} [16,21,22]. It has been suggested that the product of ideality factor (n) and zero bias barrier height measured by the $I-V$ technique Φ_{I-V} is closer to the measured Φ_{C-V} [16,23]. There is no scientific basis for such a proposal [23], however. Just as for the ideality factor, lowering of the SBH by image forces, interface states, and thermionic field emission (TFE) has frequently been invoked to explain the doping-level dependence of Φ_{I-V} [13,15,20]. Explanations of the possible origin of such anomalies have been proposed, taking into account the interface state density distribution [17,24], quantum-mechanical tunneling [3,24,25], image force lowering [25], and most recently the lateral distribution of barrier height inhomogeneities [19,26–28].

In metal semiconductor field-effect transistors (MESFETs), the performance improves as the doping concentration in the channel is increased. For a GaAs MESFET, g_m is proportional to $\sqrt{N_d}$, where N_d is the doping concentration in the channel. For digital circuits, in which enhancement type MESFETs operate with the gate biased in the forward direction, the barrier height must be sufficiently high to allow an adequate voltage swing. In this case, the forward bias gate voltage is dependent on the barrier height and ideality factor, which increases with the doping concentration. In the case of depletion type MESFETs, the performance is determined by the reverse bias voltage, which decreases very sharply with the doping concentration. In our earlier work [29], we showed that the reverse bias breakdown voltage decreased below 2.8 V when the doping concentration increased to $N_d > 1\times10^{18}\,\mathrm{cm}^{-3}$. Therefore, there is a technological importance in studying the barrier height and ideality factor as a function of doping concentration. Even the low temperature variations of barrier height and ideality factor with doping concentrations are very important for low temperature application of MESFETs. An attempt is therefore made to present the forward bias $I-V$ characteristics of Au/n-GaAs Schottky diodes in the low temperature range of 77–300 K and the concentration range of 2.5×10^{15}–$1\times10^{18}\,\mathrm{cm}^{-3}$. The doping dependence of the barrier height and the ideality factor is discussed using TFE theory as well barrier height inhomogeneities.

2. Method of analysis

In a Schottky contact, the forward bias $I-V$ relation obtained by using the TE theory is given by [25]

$$I = I_s \exp\left(\frac{q(V-IR_s)}{nkT}\right)\left[1-\exp\left(\frac{-q(V-IR_s)}{kT}\right)\right] \tag{1}$$

with

$$I_s = aA^{**}T^2\exp\left[\frac{-q\Phi_{b0}}{kT}\right], \tag{2}$$

where I_s is the saturation current (A) at zero-bias, a the diode area (cm^2), A^{**} the effective Richardson constant ($\mathrm{A/cm^2\,K^2}$), T the temperature (K), q the electronic charge (C), k is Boltzmann's constant (J/K), Φ_{b0} the zero-bias, barrier height (eV), V the forward voltage (V), n the ideality factor, and R_s the series resistance due to bulk and contact resistance (Ω). This expression is based on a combined TE-diffusion theory formulation of current flow in the diode. The $I-V$ measurements were made to determine the saturation current I_S from which the zero-bias

barrier height, Φ_{b0}, was defined in terms of the TE model, viz.,

$$\Phi_{b0} = \left(\frac{kT}{q}\right)\ln\left(\frac{aA^{**}T^2}{I_s}\right). \quad (3)$$

At a given temperature and for $V \geqslant 3kT/q$, the linear portion of the $\ln(I)$ vs. V characteristic was used to determine the saturation current (I_s) by extrapolation to zero-bias. The ideality factor was determined from the slope of the same curve. Once I_s is known, the barrier height Φ_{b0} can easily be determined from Eq. (3) at any temperature for a given diode area a and Richardson constant A^{**} ($8\,A\,cm^{-2}\,K^{-2}$ for n-type GaAs [30]).

When TFE is responsible for current transport at high doping levels, tunneling contributes to the diode current and Eq. (1) is no longer valid [13]. The forward $I-V$ characteristic in the presence of tunneling (except at very low forward bias) is described by the relation [25]

$$I = I_s \exp\left[\frac{V}{E_0}\right] \quad (4)$$

with

$$E_0 = E_{00}\coth\left[\frac{qE_{00}}{kT}\right], \quad (5)$$

where E_{00} is the tunneling parameter (also called the characteristic energy) [1,25]

$$E_{00} = \left[\frac{\hbar}{2}\right]\left[\frac{N_d}{m^*\varepsilon_s}\right]^{1/2}, \quad (6)$$

where $m^*(=m_o m_r)$ is the effective mass of electrons, $\varepsilon_s(=\varepsilon_r\varepsilon_o)$ the permittivity of the semiconductor, m_o the electron rest mass, and N_d the donor concentration in cm^{-3}. Field emission (FE) becomes important when $E_{00} \gg kT/q$, whereas TFE dominates when $E_{00} \sim kT/q$, and TE is crucial if $E_{00} \ll kT/q$. The ideality factor n is related to E_{00} through the relation [25]

$$n = \left[\frac{qE_{00}}{kT}\right]\coth\left[\frac{qE_{00}}{kT}\right]. \quad (7)$$

For a diode on low doped material, in which tunneling is absent, $n \cong 1$ (neglecting image force barrier lowering). For TFE the relation between the flat-band barrier height, Φ_0 ($=\Phi_{C-V}$), the zero-bias barrier height, Φ_{b0} ($=\Phi_{I-V}$), and the ideality factor, n, is given by [13]

$$\Phi_{b0} = \frac{\Phi_0 + \Phi_n(n-1)}{n}, \quad (8)$$

where Φ_n is the Fermi energy measured from the conduction band edge. Hence, relations (6), (7), and (8) can be used to estimate n and Φ_{b0} as a function of N_d. This approximation should be reasonably accurate for nondegenerate material but will be in error as the doping concentration exceeds about $1\times10^{18}\,cm^{-3}$ [13].

The barrier height lowering and the increase in ideality factor with decreasing measurement temperature due to the image force lowering can be understood from the following equations. The barrier lowering due to the image force is given by [31]

$$\Delta\Phi_{imf} = \left[\left(\frac{q^3N_d}{8\pi^2\varepsilon_s^3}\right)\left(\Phi_{b0} - V - \Phi_n - \frac{kT}{q}\right)\right]^{1/4}, \quad (9)$$

where

$$\Phi_n = \left(\frac{kT}{q}\right)\ln\left(\frac{N_C}{N_d}\right)$$

and V is the applied bias, and N_C the density of states at the conduction band edge ($=4.7\times10^{17}(T/300)^{3/2}$).

In principle, the increase in ideality factor with decreasing measurement temperature for all carrier concentrations might be due to image force lowering and was checked using the relation [31]

$$\frac{1}{n_{imf}} = 1 - \tfrac{1}{4}\left(\frac{q^3N_d}{8\pi^2\varepsilon_s^3}\right)^{1/4}\left(\Phi_{b0} - V - \Phi_n - \frac{kT}{q}\right)^{-3/4}. \quad (10)$$

3. Experimental details

The Schottky diodes were fabricated on epitaxial undoped and Si-doped n-type GaAs films grown on Si-doped ($2\times10^{18}\,cm^{-3}$) n+-GaAs substrates (1 0 0) 2° off towards the [1 1 0] direction using metal-organic vapor-phase epitaxy (MOVPE) and by evaporating Au under vacuum. The epitaxial films were cleaned using organic solvents and the oxide layer was removed using $HCl:H_2O$ (1 : 1) prior to the Au Schottky contact

formation. The back ohmic contacts were made using an Au–Ge eutectic with an overlayer of Au. Epitaxial n-type GaAs films of carrier concentrations in the range $2.5\,10^{15}$–$1\times10^{18}\,cm^{-3}$ were used for this study.

Room temperature $I-V$ characteristics of the diodes were checked using an automated arrangement consisting of a Keithley source measure unit (SMU236), an IBM 486 PC, and a probe station. Diodes showing similar $I-V$ characteristics at 300 K were mounted and bonded on a TO-39 header. Similar experiments were repeated on several diodes to observe the repeatability of the results. Low temperature $I-V$ characteristics for carrier concentrations of 2.5×10^{15}, 1×10^{17} and $1\times10^{18}\,cm^{-3}$ were obtained in the temperature range of 77–300 K using the automated setup described above coupled with a cryostat. The temperature was within ±1 K during the data acquisition. The carrier concentration and flat-band barrier height were determined using the reverse bias $C-V$ characteristics measured at 1 MHz on a HP4194A LCR bridge. Electrochemical capacitance–voltage (ECV) profiling further confirmed the carrier concentration. The barrier height and the ideality factor were simulated using Eqs. (6)–(8).

4. Results and discussion

The current density vs. voltage ($J-V$) characteristics of the Schottky diodes at concentrations of (a) $2.5\times10^{15}\,cm^{-3}$, (b) $1\times10^{17}\,cm^{-3}$ and (c) $1\times10^{18}\,cm^{-3}$ are plotted as a function of temperature in Figs. 1(a)–(c), respectively. The plots exhibit a linear portion over 3–4 decades of magnitude of current density. The diode ideality factor n, the saturation current I_s, and the zero-bias barrier height Φ_{b0} were determined using Eqs. (1) and (3).

The zero-bias barrier height and ideality factor are plotted as a function of temperature at three different concentrations in Fig. 2. The plot shows that the ideality factor increases with decreasing temperature and that the change is more pronounced below 150 K, whereas the zero-bias barrier height decreases with decreasing temperature except at $2.5\times10^{15}\,cm^{-3}$. For this concentration, the barrier height first increases with decreasing temperature up to 160 K and then decreases. This apparent decrease in the zero-bias barrier height below 160 K is similar to the observations made by others on different types of Schottky diodes [9,11,14,18,26,32]. The experimental barrier heights and ideality factors, as well as those simulated using two different models, are shown in Table 1. From Fig. 2 it is seen that the calculated curves, using Eqs. (6)–(8) with the barrier height determined from $C-V$ measurement for each doping level, lie higher than the measured value of Φ_{b0}; the opposite is true for the ideality factor n. This may be partly due to the neglect of the image force in the calculation, and a further deviation may be caused by a thin film of thermal oxide formed [33] on the samples during the time elapsed between etching and deposition of the diodes. However, calculated barrier height using Eqs. (6)–(8) with the barrier height determined from $C-V$ measurement along with the barrier height lowering due to TFE and ideality factor at doping concentration of $1\times10^{18}\,cm^{-3}$ fit the TFE theory very well. The barrier height lowering due to TFE is much more significant at doping concentration of $1\times10^{18}\,cm^{-3}$ than at lower doping level and hence, it has been added to the calculated barrier height. Because the $I-V$ measurement technique is sensitive to the barrier-lowering effect, the effective $I-V$ barrier height is dependent on the applied voltage and on the doping level of the film. The barrier-lowering mechanism includes the effects of the image force, the effects of tunneling current through the potential barrier, and an alteration of the charge distribution near the interface [34].

4.1. Effect of image force

In order to understand the factors influencing the lowering of the barrier height with increasing concentration and decreasing temperature, the effect of image force lowering was considered. The value of $\Delta\Phi_{imf}$ using Eq. (9) is 13.85 meV for a Φ_{b0} of 0.89 eV at a carrier concentration of $2.5\times10^{15}\,cm^{-3}$; 34.6 meV for a Φ_{b0} of 0.854 V at a concentration of $1\times10^{17}\,cm^{-3}$; and 57.63 meV

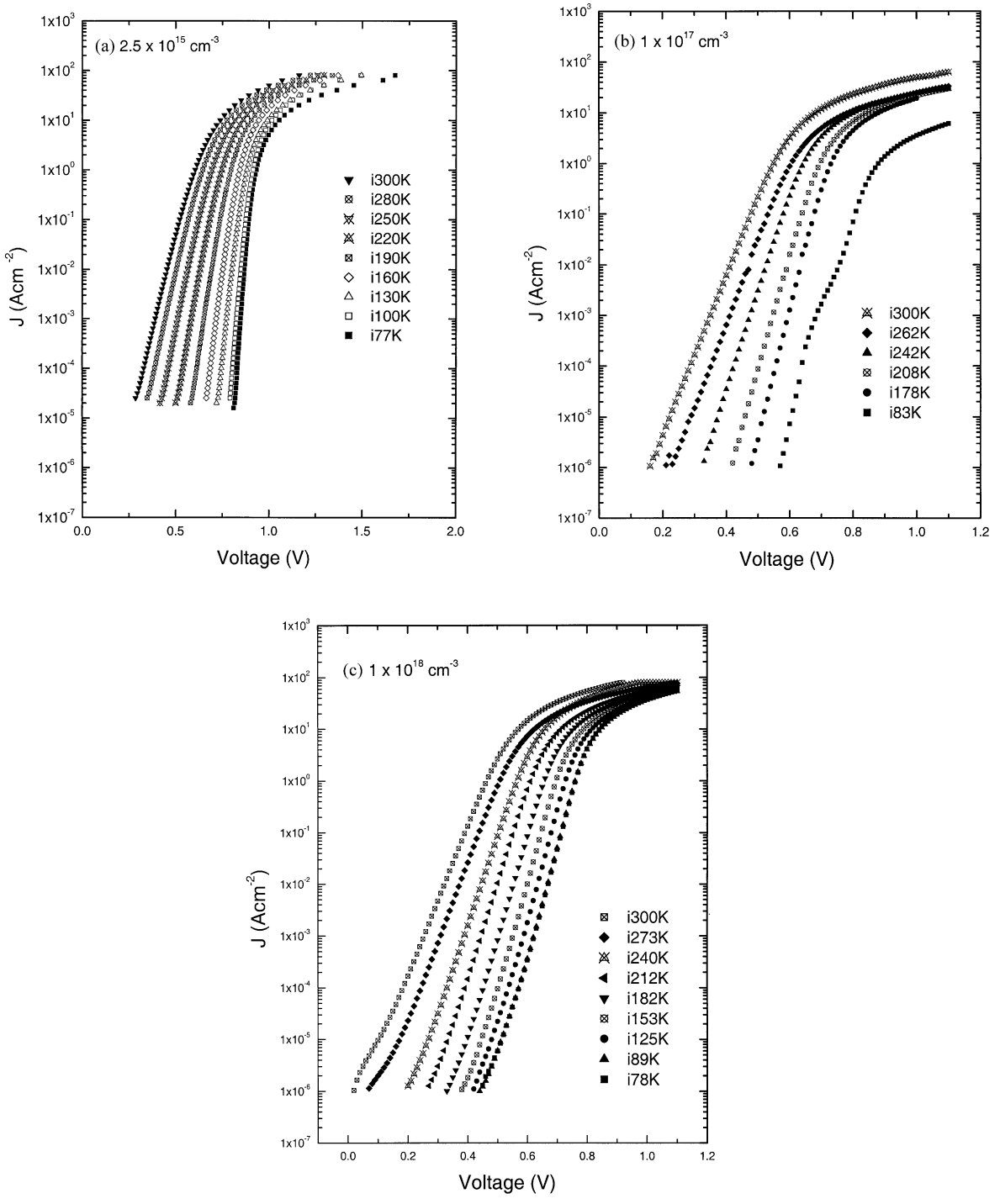

Fig. 1. The current density vs. voltage characteristics of Au/n-GaAs Schottky diodes at various temperatures and doping concentrations: (a) $N_d = 2.5 \times 10^{15}\,cm^{-3}$, (b) $N_d = 1 \times 10^{17}\,cm^{-3}$, (c) $N_d = 1 \times 10^{18}\,cm^{-3}$.

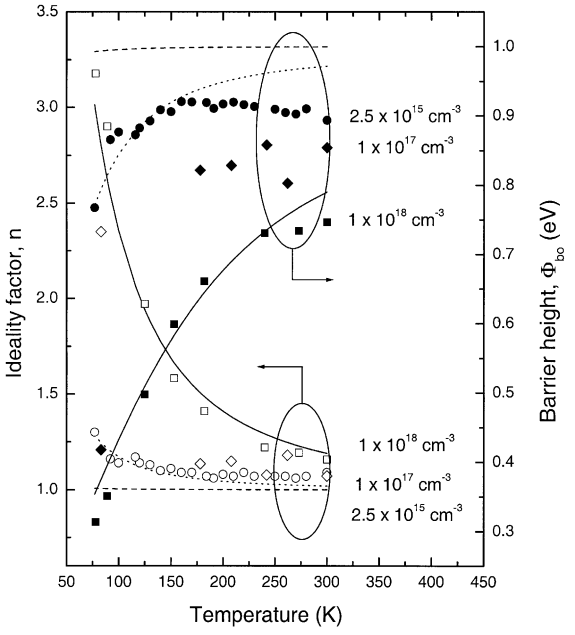

Fig. 2. Measured barrier heights and ideality factors of Au/n-GaAs Schottky diodes vs. temperature: (a) effective barrier height and (b) ideality factor. The calculated lines (---: $2.5\times10^{15}\,\mathrm{cm}^{-3}$; ···: $1\times10^{17}\,\mathrm{cm}^{-3}$; —: $1\times10^{18}\,\mathrm{cm}^{-3}$) represent an approximation based on TFE theory.

for a Φ_{b0} of 0.746 eV at a concentration of $1\times10^{18}\,\mathrm{cm}^{-3}$. All cases are evaluated for a typical forward bias voltage of 0.45 V at 77 K. This value of $\Delta\Phi_{imf}$ is much lower at all carrier concentrations than the observed barrier lowering of 126 meV at $2.5\,10^{15}\,\mathrm{cm}^{-3}$, 436 meV at $1\times10^{17}\,\mathrm{cm}^{-3}$, and 433 meV at $1\times10^{18}\,\mathrm{cm}^{-3}$, respectively. Therefore, the image force effect alone cannot account for the lowering of the barrier height.

The evaluation of the ideality factor from Eq. (10) yields values of 1.011, 1.025, and 1.051 at 300 K and 1.008, 1.022, and 1.045 at 77 K, using a typical bias value of 0.45 V for the concentrations 2.5×10^{15}, 1×10^{17}, and $1\times10^{18}\,\mathrm{cm}^{-3}$, respectively. There is hardly any change of ideality factor between the two measurement temperatures of 300 and 77 K using Eq. (10). This shows that the observed variation in the ideality factor cannot be explained by image force lowering.

4.2. Effect of thermionic field emission

The decrease in barrier height and the increase in ideality factor with a decrease in the temperature are indicative of a deviation from the pure TE theory, and one thus must consider the TFE mechanism. The E_{00} parameter determines the conduction mechanism, whether it is by TE, TFE, or FE. The value of E_{00} is 1.0 meV at $2.5\times10^{15}\,\mathrm{cm}^{-3}$, 6.317 meV at $1\times10^{17}\,\mathrm{cm}^{-3}$, and 19.97 meV at $1\times10^{18}\,\mathrm{cm}^{-3}$. According to the theory, TFE dominates only when $E_{00}\sim kT$. The value of E_{00} calculated from Eq. (6) is less than kT by a factor of six even at 77 K for a concentration of $2.5\times10^{15}\,\mathrm{cm}^{-3}$. The value of E_{00} is less than kT for a concentration of $1\times10^{17}\,\mathrm{cm}^{-3}$. For a concentration of $1\times10^{18}\,\mathrm{cm}^{-3}$, the value of E_{00} is greater than kT only at temperatures below 240 K. The FE dominates only when $E_{00}\gg kT/q$; for a concentration of $1\times10^{18}\,\mathrm{cm}^{-3}$ FE behavior is observed below 240 K only. The barrier height lowering for TFE, determined using the theoretically calculated value of E_{00} for all carrier concentrations, is given by [25]

$$\Delta\Phi_{TFE}=\left(\frac{3}{2}\right)^{2/3}E_{00}^{2/3}V_{d}^{1/3}, \tag{11}$$

where V_d is the built-in potential. Table 2 shows the calculated values of $\Delta\Phi_{TFE}$ at different concentrations and at 300 K.

The ideality factor is further analyzed by considering the variation in the ideality factor caused by a tunneling current. The relation for the variation in the ideality factor is given by Eq. (7). The intercept on the E_0 ($=nkT/q$) axis of Fig. 3 yields the value of E_{00} for the Schottky diode under study. It can be seen from Fig. 3 that the experimental points for a carrier concentration of $2.5\times10^{15}\,\mathrm{cm}^{-3}$ are linear. Line 1, corresponding to a carrier concentration of $2.5\times10^{15}\,\mathrm{cm}^{-3}$, does not pass through the origin, thus implying a higher characteristic energy (E_{00}), which cannot be explained by the above theories. In order to confirm the higher value of the characteristic energy, another method was used which requires plotting of the theoretically determined values of $1/n$ vs. $1000/T$ plot (Fig. 4) [31]. The following relation was used to generate such theoretical plots

Table 1
The experimental and simulated barrier heights and ideality factors at different temperatures and concentrations

T (K)	n_{expt}	Φ_{b0}expt (eV)	Werner & Güttler Equ.		TFE theory	
			n_{sim}	Φ_{b0}sim (eV)	n_{sim}	Φ_{b0}sim (eV)
$2.5\times10^{15}\,cm^{-3}$						
300	1.09	0.893	1.058	0.967	1.00	0.999
280	1.07	0.910	1.062	0.953	1.00	0.999
270	1.06	0.902	1.064	0.951	1.00	0.999
260	1.07	0.904	1.066	0.948	1.00	0.999
250	1.07	0.909	1.069	0.946	1.00	0.999
230	1.07	0.913	1.075	0.940	1.00	0.999
220	1.09	0.916	1.078	0.937	1.00	0.999
210	1.07	0.919	1.081	0.933	1.001	0.999
200	1.08	0.917	1.086	0.930	1.001	0.999
191	1.06	0.910	1.090	0.926	1.001	0.998
184	1.07	0.918	1.093	0.922	1.001	0.998
170	1.09	0.919	1.101	0.915	1.001	0.998
160	1.09	0.920	1.108	0.909	1.001	0.998
150	1.11	0.906	1.115	0.902	1.002	0.998
140	1.1	0.908	1.124	0.894	1.002	0.997
130	1.13	0.892	1.134	0.885	1.002	0.997
120	1.14	0.882	1.146	0.874	1.003	0.997
116	1.17	0.872	1.152	0.970	1.003	0.997
100	1.14	0.876	1.179	0.847	1.004	0.996
92	1.16	0.865	1.197	0.833	1.005	0.995
77	1.30	0.764	1.243	0.798	1.007	0.993
$1\times10^{17}\,cm^{-3}$						
300	1.072	0.854	1.1198	0.851	1.019	0.972
262	1.180	0.803	1.1359	0.845	1.026	0.966
242	1.077	0.858	1.1466	0.840	1.030	0.962
208	1.149	0.828	1.1702	0.830	1.040	0.952
178	1.136	0.821	1.20	0.818	1.055	0.946
83	2.350	0.418	1.5026	0.725	1.245	0.794
$1\times10^{18}\,cm^{-3}$						
300	1.158	0.746	1.246	0.740	1.190	0.790
273	1.194	0.734	1.274	0.724	1.232	0.767
240	1.221	0.730	1.319	0.705	1.290	0.733
182	1.410	0.660	1.455	0.650	1.486	0.645
153	1.583	0.599	1.582	0.606	1.664	0.583
125	1.971	0.497	1.805	0.545	1.941	0.510
89	2.900	0.351	2.620	0.409	2.623	0.395
78	3.177	0.314	3.363	0.342	2.976	0.357

with E_{00} as the parameter

$$\frac{1}{n}=\frac{kT(1-\beta)}{qE_0}, \tag{12}$$

where β indicates the bias dependence of the barrier height. Since the values of $1/n$ are sensitive to changes near unity, such a plot provides a good check to determine whether the dominating mechanism is TE or TFE. The experimentally determined values of the ideality factor are superimposed on such a plot (Fig. 4) to approximately determine the values of E_{00} and β. It is observed

Table 2
Schottky diodes parameters for the investigated epitaxial layers at 300 K

N_d (cm^{-3})	E_{00} (meV)	n	V_d (V)	Φ_{b0}expt (eV)	$\Delta\Phi_{TFE}$ (meV)	$\Phi_{b0}+\Delta\Phi_{TFE}$ (eV)	σ_s	Φ_{bmean} (eV)	α	Σ
2.50×10^{15}	1.00	1.090	0.910	0.893	12.70	0.906	0.053	1.012	0.006	0.024
3.00×10^{16}	3.46	1.060	0.867	0.867	26.54	0.894	—	—	—	—
1.00×10^{17}	6.32	1.072	0.854	0.854	42.50	0.896	0.050	0.900	0.020	0.045
1.30×10^{17}	7.20	1.100	0.844	0.844	42.75	0.886	—	—	—	—
2.00×10^{17}	8.93	1.080	0.836	0.836	49.20	0.885	—	—	—	—
6.65×10^{17}	16.29	1.134	0.775	0.775	71.09	0.846	—	—	—	—
1.00×10^{18}	19.97	1.158	0.746	0.746	87.50	0.834	0.085	0.880	0.020	0.054

that the experimental points closely match the curve with $E_{00}=6.5\,\text{meV}$ and $\beta=0.032$ for a doping concentration of $2.5\times10^{15}\,\text{cm}^{-3}$. We followed a similar procedure for the other doping concentrations to determine the values of E_{00} and β. Fig. 5 shows the experimental and calculated values of E_{00} (using Eq. (6)) as a function of doping concentration N_d. From this figure one finds that the observed value of E_{00} is higher than the calculated one. This indicates that the conduction mechanism is TFE even in the limit of low doping concentration, despite the fact that one

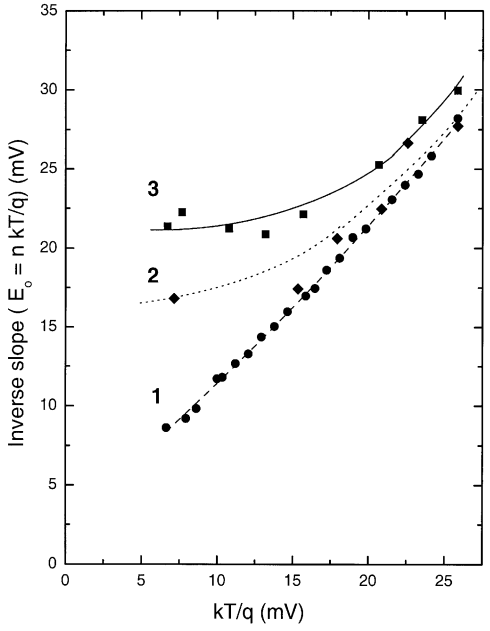

Fig. 3. Plot of inverse slope (E_0) vs. kT/q showing the temperature dependence of ideality factor. Line 1 ($2.5\times10^{15}\,\text{cm}^{-3}$) shows the possibility of a higher characteristic energy than that predicted by the TE theory and estimated using Eq. (6). Line 2 ($1\times10^{17}\,\text{cm}^{-3}$) and 3 ($1\times10^{18}\,\text{cm}^{-3}$) represent the behavior when conduction mechanism is dominated by TFE. Lines 2 and 3 are drawn to show the trend and do not represent any theoretical fit.

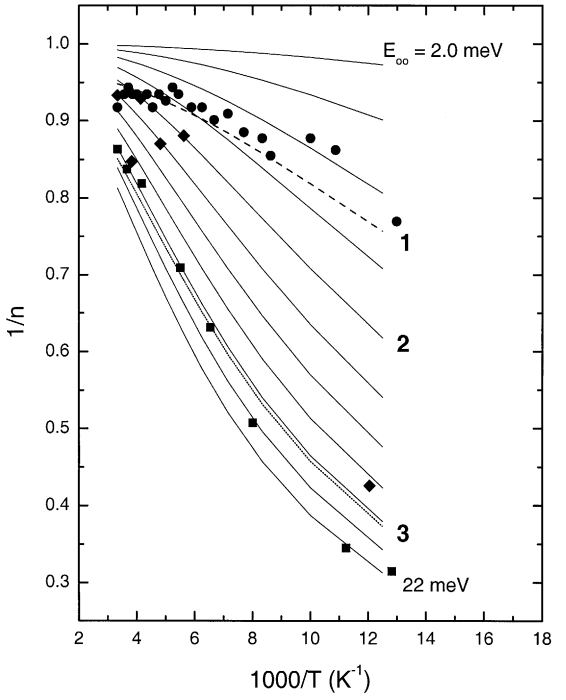

Fig. 4. Plot showing $1/n$ vs. $1/T$ curves (solid lines) with E_{00} as a parameter ranging from 2 to 22 meV in steps of 2 meV generated by Eq. (12) and $\beta=0$. The experimental points are also superimposed on the theoretically generated plot. Lines 1 (●: $2.5\times10^{15}\,\text{cm}^{-3}$; 2 (◆: $1\times10^{17}\,\text{cm}^{-3}$); and 3 (■: $1\times10^{18}\,\text{cm}^{-3}$) shown on the plot represents a curve with the value of $E_{00}=6.5\,\text{meV}$ and $\beta=0.032$; $E_{00}=10\,\text{meV}$ and $\beta=0$; and $E_{00}=18\,\text{meV}$ and $\beta=0.016$, respectively.

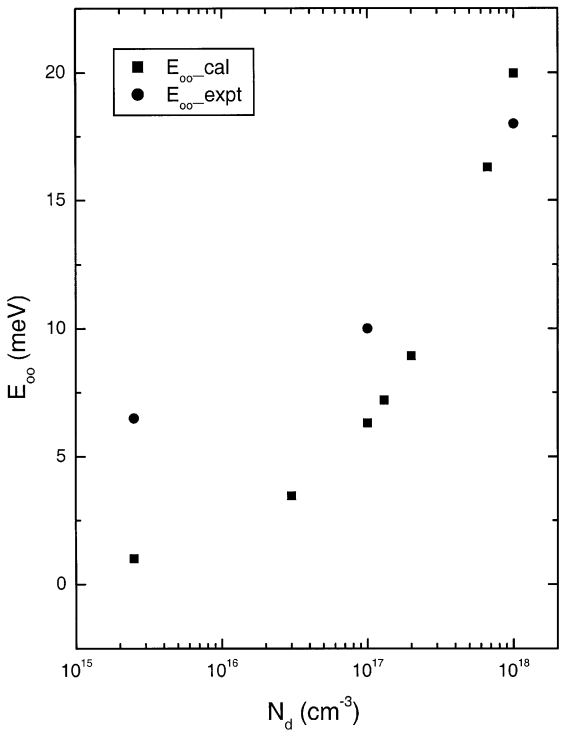

Fig. 5. Plot showing the calculated E_{00} using Eq. (6) with the experimental value in the concentration range of 2.5×10^{15}–$1.0\times10^{18}\,\mathrm{cm}^{-3}$.

would expect it to be within the domain of the TE conduction mechanism. Therefore, the diode having a doping concentration of $2.5\times10^{15}\,\mathrm{cm}^{-3}$ exhibits high characteristic energy not expected for this concentration, implying a conduction mechanism dominated by TFE (instead of TE) at low temperatures. The origin of such high characteristic energy was not predicted by the simple theory; rather, it has been attributed to several effects. The parameter E_{00} is affected by the electric field at the semiconductor surface and the density of states at the semiconductor surface. Any mechanism such as the geometrical inhomogeneities arising due to crystal defects, surface roughness near the device periphery, local pile up of dopants, the presence of a relatively thick insulating interfacial layer with low dielectric constant, and charge in the interfacial layer, could possibly increase the electric field near the semiconductor surface [32]. Multistep tunneling through the interface states also yields a higher characteristic energy [35].

The measured barrier heights and ideality factors vs. doping concentration at 300 K are shown in Figs. 6(a) and (b), respectively. Considering first Fig. 6(a), we see that the continuous line, representing an approximation based on TFE theory using Eqs. (6)–(8) with the homogeneous barrier height $\Phi_0 = 0.97\pm0.08\,\mathrm{eV}$, lies higher than the measured value of Φ_{b0}. The effect of barrier height lowering (neglecting the image force effect on barrier lowering) due to TFE was added to the measured value of barrier height (Φ_{b0}) using TE theory and re-plotted in Fig. 6(a). It is seen from Fig. 6(a) that the effective barrier heights fit well with the calculated curve. From this figure it is also seen that the barrier height determined from the $C-V$ measurement decreases from 1.02 to 0.84 eV as the carrier concentration increases from 2.5×10^{15} to $1\times10^{18}\,\mathrm{cm}^{-3}$. Ideally, the barrier height determined from the $C-V$ measurement should be the same for all doping levels. The observed effect could be due to the presence of an interfacial layer [33,36] and by the change of the dopant concentration near the metal-semiconductor (MS) interface [37].

We have included a few results presented by other workers in GaAs as well as in Si Schottky diodes for comparison [15,34,36] in Fig. 6(a). Newman et al. studied the electrical transport characteristics of nine metals on n-GaAs [34] and n-InP [38] as a function of doping level on (1 1 0) surfaces. However, only results from Au/n-GaAs Schottky diodes have been included in Fig. 6(a). One finds from Fig. 6(a) that our results agree well with the results presented by Newman et al. [34] and Horvath et al. [36] with their $C-V$ measurement result. However, the barrier height determined from $I-V$ characteristics measured by Horvath et al. [36] is far below our results. They pointed out that this could be due to excess current flow through the diodes and by the incorrect value of the Richardson constant used for the evaluation of Φ_{b0}. The decrease in barrier height with increasing dopant concentration is due to the effect of the interfacial layer and interface states [36]. The barrier height determined from the $I-V$ and $C-V$ measurements for palladium-silicide

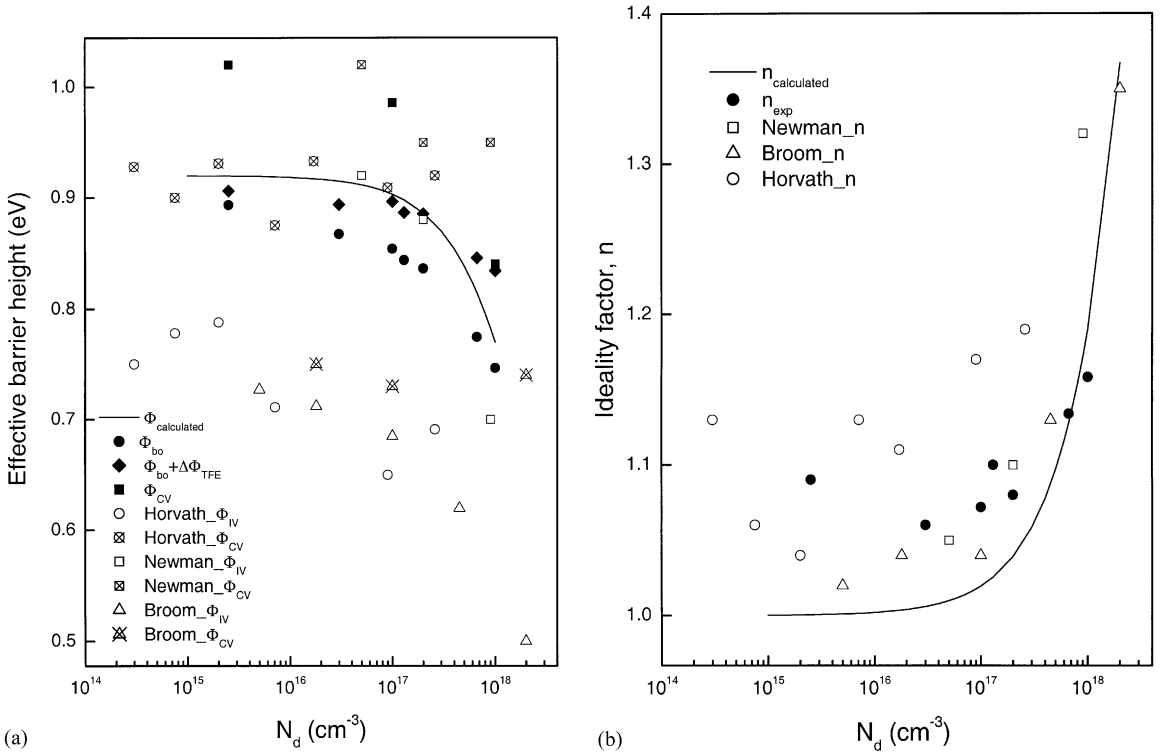

Fig. 6. (a) Measured barrier heights of Au/n-GaAs Schottky diodes vs. doping concentration at 300 K. The continuous lines represent an approximation based on TFE theory. The symbols are meaning ● = Φ_{b0} and ◆ = $\Phi_{b0} + \Delta\Phi_{TFE}$. (b) Measured ideality factors of Au/n-GaAs Schottky diodes vs. doping concentration at 300 K. The continuous lines represent an approximation based on TFE theory.

Schottky diodes [15] are also included in Fig. 6(a). Weitering et al. [39] studied the $I-V$ characteristics of Ag Schottky diodes on n- and p-type Si in the doping concentration range of 3×10^{14}–$3\times10^{17}\,cm^{-3}$ on different surfaces. They found that the barrier heights are spatially non-uniform and concluded that this might be due to structural and morphological inhomogeneities at the interface.

The ideality factor increases with the increasing carrier concentration and can be seen from Fig. 6(b). The continuous lines, representing an approximation based on TFE theory using Eqs. (6) and (7) lie lower than the measured value of n. We have included a few results presented by other workers in GaAs as well as in Si Schottky diodes for comparison [15,34,40] in Fig. 6(b). The experimental ideality factor is higher than the calculated value may be caused by a thin film of oxide layer on the samples during the time elapsed between etching and deposition of the metal. Even the ideality factor measured by Horvath et al. [40] is higher than our results and it is also far from the calculated curve. The agreement is good between the experimental and calculated values of the ideality factors in the high doping levels. However, Broom et al. [15] found that the agreement is generally good in the lower carrier concentration except at the highest doping where tunneling plays a significant role in the current transport. The results are well described in our case by TFE theory.

4.3. Effect of barrier height inhomogeneity

Werner and Güttler [26] proposed that the barrier height has a Gaussian distribution characterized by a mean barrier height. The reduction

in barrier height with temperature may be explained by the lateral distribution of the barrier height. The assumption of the Gaussian distribution for the barrier height yields the following equation for the barrier height [26]

$$\Phi_{b0} = \Phi_{bmean} - \left(\frac{\sigma_s^2}{2kT}\right), \tag{13}$$

where Φ_{b0} is the zero-bias barrier height, Φ_{bmean} the mean barrier height, and σ_s the standard deviation of the barrier distribution. The mean barrier height is the same as the barrier height measured by a capacitance–voltage measurement, which is essentially the barrier height at zero electric field. Since the flat-band barrier height, $\Phi_{b0}^{f} = n\Phi_{b0} - (n-1)kT\ln(N_C/N_d)$ is also obtained at zero electric field, both of the quantities are the same [6]. Using this relation and $\Phi_{b0}^{f} = \Phi_{bmean}$, the values of σ_s and Φ_{bmean} are calculated and are tabulated in Table 2. Using the values of σ_s and Φ_{b0} from Table 2 and Eq. (13), a continuous curve was generated as a function of operating temperature and concentration, which is plotted in Fig. 7. It may be observed from this figure that although the curve obtained using Eq. (13) agrees well with the values of the zero-bias barrier height in the 77–210 K range, it deviates appreciably from the experimental points at higher temperatures for a concentration of $2.5\times10^{15}\,cm^{-3}$. Also it can be seen from this figure that the curve agrees very well for the other concentrations, in particular $1\times10^{18}\,cm^{-3}$.

Using the potential fluctuations model [26], the ideality factor is given by the relation

$$\frac{1}{n} = 1 - \alpha + \frac{\sigma_s q\Sigma}{kT}. \tag{14}$$

Using the experimentally determined values of n at different temperatures and the value of σ_s obtained from Eq. (13), the values of α and Σ were obtained. These values can also be seen from Table 2. The experimentally determined values and the continuous curve representing a fit to these values using the parameters obtained using Eq. (14) are shown in Fig. 7. From this figure it is also seen that the potential fluctuation model agrees well with the above concentrations.

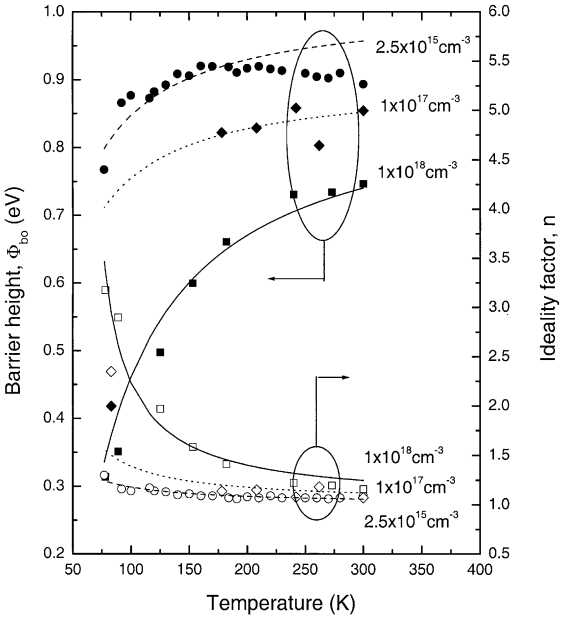

Fig. 7. Variation in zero-bias barrier height and ideality factor with temperature at different doping concentrations. The lines (---: $2.5\times10^{15}\,cm^{-3}$; ⋯: $1\times10^{17}\,cm^{-3}$; —:$1\times10^{18}\,cm^{-3}$) are generated using Eqs. (13) and (14).

Sullivan et al. [27] and Tung [17] proposed another approach to lateral inhomogeneities in the Schottky barrier. They proposed that the Schottky barrier consists of laterally inhomogeneous patches of different barrier heights. The patches with lower barrier height yield a larger ideality factor and vice versa. Schmitsdrof et al. [28] found a linear correlation between the zero-bias barrier height and the ideality factors using Tung's [17] theoretical approach. The extrapolation of the linear fit to this data yields the homogeneous barrier height at an ideality factor of 1.01. A similar analysis of our data to this effect is presented in Fig. 8 for a concentration of $2.5\times10^{15}\,cm^{-3}$. It is observed that the barrier height correlates linearly with the ideality factors measured at temperatures below 200 K. The homogeneous barrier height determined from this analysis yields a value of 0.97 ± 0.08 eV for a concentration of $2.5\times10^{15}\,cm^{-3}$. This homogeneous barrier height is in close agreement with the effective barrier height ($\Phi_{b0}^{C-V} = 1.02$ eV) obtained from the $C-V$ measurement. According to

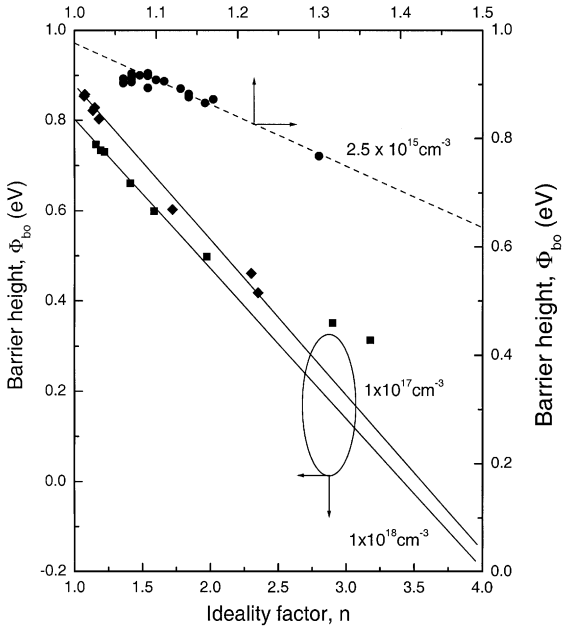

Fig. 8. The zero-bias barrier height vs. ideality factor at different temperatures and doping concentrations. The extrapolation of the linear fit to the points below 200 K yields a homogeneous barrier height value of 0.97 eV at doping level of $2.5 \times 10^{15}\,\mathrm{cm}^{-3}$.

Schmitsdroff et al. [28], the larger the discrepancy between the homogeneous barrier height and the effective barrier height, the poorer the quality of the grown layer. A homogeneous barrier height of 0.896 ± 0.08 eV ($\Phi_{b0}^{C-V} = 0.986$ eV) was obtained from $I-V$ measurements for a doping level of $1 \times 10^{17}\,\mathrm{cm}^{-3}$. Similarly, a homogeneous barrier height of 0.809 ± 0.08 eV ($\Phi_{b0}^{C-V} = 0.84$ eV) was obtained from $I-V$ measurements for a doping level of $1 \times 10^{18}\,\mathrm{cm}^{-3}$. This lowered barrier height for the higher doping level of $1 \times 10^{18}\,\mathrm{cm}^{-3}$ was observed and it may be attributed to the tunneling effect. Since the barrier heights were calculated using the assumption of TE only, the additional tunnel current leads to an estimated barrier height lower than the true value. The experimental barrier heights obtained from $C-V$ measurements are much lower for the higher doping concentration as compared to lower concentration. Such dependence on the doping level can be expected due to the electric field dependence of the dipole layer between the semiconductor and the metal.

5. Conclusions

The forward $I-V$ characteristics of Au/n-GaAs Schottky diodes were measured in the temperature range of 77–300 K for three different doping concentrations. The $I-V$ characteristics were strongly dependent on the doping concentration. The zero-bias barrier height decreased and the ideality factor increased with decreasing temperature and increasing doping concentration; the changes are quite significant at low temperatures. The significant decrease in barrier height and increase in ideality factor at low temperatures and high doping concentrations can be explained by thermionic field-emission theory. The doping dependence of the barrier height and the ideality factor were obtained in the concentration range of 2.5×10^{15}–$1.0 \times 10^{18}\,\mathrm{cm}^{-3}$, and the results are well described using TFE theory. According to Tung's approach of lateral inhomogeneities, the homogeneous barrier height and the effective barrier heights are closely matched, which demonstrates the good quality of the GaAs films. The barrier height inhomogeneities at the interface also explain the results of barrier height and ideality factor change at low temperatures at all doping concentrations.

References

[1] F.A. Padovani, R. Stratton, Solid State Electron. 9 (1966) 695.
[2] F.A. Padovani, G. Sumner, J. Appl. Phys. 36 (1965) 3744.
[3] F.A. Padovani, in: R.K. Willardson, A.C. Beer (Eds.), Semiconductors and Semimetals, Vol. 7A, Academic Press, New York, 1971.
[4] F. Chekir, G.N. Lu, C. Barret, Solid State Electron. 29 (1986) 519.
[5] J.H. Werner, Appl. Phys. A 47 (1989) 291.
[6] L.F. Wagner, R.W. Young, A. Sugerman, IEEE Electron. Device Lett. EDL-4 (1983) 320.
[7] C.T. Chuang, Solid State Electron. 27 (1984) 299.
[8] Zs.J. Horvath, A. Bosacchi, S. Franchi, E. Gombia, R. Mosca, A. Motta, Mater. Sci. Eng. B 28 (1994) 429.
[9] S. Chand, J. Kumar, Appl. Phys. A 63 (1996) 171.
[10] P. Cova, A. Singh, Solid State Electron. 33 (1990) 11.
[11] K. Shenai, R.W. Dutton, IEEE Trans. Electron. Devices ED-35 (1988) 468.
[12] Y.P. Song, R.L. Van Meirhaeghe, W.H. Laflere, F. Cardon, Solid State Electron. 29 (1986) 633.

[13] R.F. Broom, H.P. Meier, W. Walter, J. Appl. Phys. 60 (1986) 1832.
[14] A.S. Bhuiyan, A. Martinez, D. Esteve, Thin Solid Films 161 (1988) 93.
[15] R.F. Broom, Solid State Electron. 14 (1971) 1087.
[16] V.W.L. Chin, M.A. Green, J.W.V. Storey, J. Appl. Phys. 68 (1990) 3470.
[17] R.T. Tung, Phys. Rev. B 45 (1992) 13509.
[18] R. Hackam, P. Harrop, IEEE Trans. Electron. Devices ED-19 (1972) 1231.
[19] R.T. Tung, J.P. Sullivan, F. Schrey, Mater. Sci. Eng. B 14 (1992) 266.
[20] R.J. Archer, T.O. Yep, J. Appl. Phys. 41 (1970) 303.
[21] N. Newman, M.V. Schilfgaarde, T. Kendelwicz, M.D. Williams, W.E. Spicer, Phys. Rev. B 33 (1986) 1146.
[22] A. Thanailakis, A. Rasul, J. Phys. C 9 (1976) 337.
[23] R. Hackman, P. Harrop, Solid State Commun. 11 (1972) 669.
[24] C.R. Crowell, Solid State Electron. 20 (1977) 171.
[25] E.H. Rhoderick, R.H. Williams, Metal-Semiconductor Contacts, Clarendon, Oxford, 1988.
[26] J.H. Werner, H. Guttler, J. Appl. Phys. 69 (1991) 1522.
[27] J.P. Sullivan, R.T. Tung, M.R. Pinto, W.R. Graham, J. Appl. Phys. 70 (1991) 7403.
[28] R.F. Schmitsdrof, T.U. Kampen, W. Mönch, J. Vac. Sci. Technol. B 15 (1997) 1221.
[29] M.K. Hudait, S.B. Krupanidhi, Solid State Electron. 43 (1999) 2135.
[30] C.R. Crowell, Solid State Electron. 8 (1965) 395.
[31] M. Wittemer, Phys. Rev. B 42 (1990) 5249.
[32] Zs.J. Horvath, Mater. Res. Soc. Symp. Proc. 260 (1992) 359.
[33] S. Hardikar, M.K. Hudait, P. Modak, S.B. Krupanidhi, N. Padha, Appl. Phys. A 68 (1999) 49.
[34] N. Newman, M.V. Schilfgaarde, T. Kendelwicz, M.D. Williams, W.E. Spicer, Phys. Rev. B 33 (1986) 1146.
[35] P.L. Hansclaer, W.H. Laflere, R.L.V. Meirhaeghe, F. Cardon, J. Appl. Phys. 56 (1984) 2309.
[36] Zs.J. Horvath, I. Gyuro, M.N. Sallay, P. Tutto, Vacuum 40 (1990) 201.
[37] Zs.J. Horvath, J. Appl. Phys. 64 (1988) 443.
[38] N. Newman, T. Kendelewicz, L. Bowman, W.E. Spicer, Appl. Phys. Lett. 46 (1985) 1176.
[39] H.H. Weitering, J.P. Sullivan, R.J. Carolissen, W.R. Graham, R.T. Tung, Appl. Surf. Sci. 70/71 (1993) 422.
[40] Zs. J. Horvath, I. Gyuro, M. Nemeth-Sallay, P. Tuto, A. Nagy, L. Dozsa, B. Kovacs, E.K. Pal, B. Szentpali, A. Fogt, T. Nemeth, G. Stubnya, A. Nemcsics, Proceedings of the 7th Czechoslovak Conference on Electronics and Vacuum Physics, Bratislava, September 3–6, 1985, p. 747.